Appl. Phys. B (2013) 112:143–152
DOI 10.1007/s00340-013-5383-8

Applied Physics B
Lasers and Optics

Metamaterial polarization converter analysis: limits of performance

Dmitry L. Markovich · Andrei Andryieuski · Maksim Zalkovskij · Radu Malureanu · Andrei V. Lavrinenko

Received: 17 January 2013 / Accepted: 16 February 2013 / Published online: 8 March 2013

Abstract In this paper, we analyze the theoretical limits of a metamaterial-based converter with orthogonal linear eigenpolarizations that allow linear-to-elliptical polarization transformation with any desired ellipticity and ellipse orientation. We employ the transmission line approach providing a needed level of the design generalization. Our analysis reveals that the maximal conversion efficiency for transmission through a single metamaterial layer is 50 %, while the realistic reflection configuration can give the conversion efficiency up to 90 %. We show that a double layer transmission converter and a single layer with a ground plane can have 100 % polarization conversion efficiency. We tested our conclusions numerically reaching the designated limits of efficiency using a simple metamaterial design. Our general analysis provides useful guidelines for the metamaterial polarization converter design for virtually any frequency range of the electromagnetic waves.

1 Introduction

Metamaterials provide new exciting possibilities for light wave manipulations especially with operations on the wave polarization, which are on demand not only in the optical and microwave range, but also in the booming field of terahertz (THz) science and technology, due to the natural limitations of the material properties. THz waves have high potential in communication systems, food quality control, defense, biomedical imaging and chemical spectroscopy [1, 2, 3]. For some THz applications, for example, magneto-optical spectroscopy [4], it is desirable to have a circularly or elliptically polarized wave, while most THz sources generate linearly polarized radiation.

There are two main routes to get the polarization rotation or conversion. The "phase" route is to introduce eigenwaves phase offsets in birefringent or gyrotropic media with approximately equal transmitted amplitudes. The "amplitude" route is to play with transmission coefficients for the eigenwaves letting the output to have a polarization state of the dominating eigenwave. The unnecessary polarization is then discriminated by the higher absorption and/or higher reflection of another eigenstate. Two illustrative examples of these routes in the THz range are an achromatic quarter-wave plate made from quartz [5] and a giant Faraday effect in an electron plasma in n-InSb semiconductor [6]. Being broadband, these solutions, however, claim extended sizes (3 cm) of devices in the former case and intense magnetic fields of several tesla in the latter.

In the contrary to the aforementioned bulk devices, the metamaterial (metasurfaces, frequency selective surfaces)-based solutions can be extremely compact, for example, a single thin layer can be enough to get the required polarization state without external magnetic field. Several metamaterial-based polarization conversion devices have already been proposed, which can be tentatively grouped by the operational principle and configuration: birefringent polarizers [7, 8], transmission [9– 16] and reflection [17–21] polarizers based on resonant particles or slits and chiral

D. L. Markovich (✉)
Department of Photonics and Information Technology, St. Petersburg National Research University of Information Technologies, Mechanics and Optics, 197101 St. Petersburg, Russian Federation
e-mail: dmmrkovich@gmail.com

A. Andryieuski · M. Zalkovskij · R. Malureanu · A. V. Lavrinenko
Department of Photonics Engineering, Technical University of Denmark, Ørsteds pl. 343, 2800 Kongens Lyngby, Denmark

metamaterials [22–27]. Some of the proposed devices have drawbacks, for example, being based on resonant inclusions, apertures or meta-atoms they usually exhibit a narrow bandwidth or convert a linear polarization into the specific circular one. Nevertheless, such big variety of converters' designs pose the question on whether the natural bounds for the conversion efficiency exist and how it is possible to approach them from the practical point of view.

In this contribution, we evaluate the theoretical limits of the efficiency of polarization converters based on metamaterial with linear orthogonal eigen polarizations. We consider the case of conversion of a linear polarization into any elliptical one with a desired ellipticity and ellipse orientation. We employ the transmission line theory, which proved to be useful in the theory of metamaterials [28]. Two principle experimental configurations are considered: reflection and transmission at normal incidence. We show that the conversion efficiency can be virtually as high as 50 % for one transmission layer and up to full 100 % for a polarization converter with two layers. In the reflection configuration even with only one layer conversion of up to 80–90 % is feasible, while one layer with a ground plane can give 100 % conversion with the relaxed requirements on the metamaterial unit cell design. Demonstration is exemplified on the THz range devices, as effective metamaterials circular polarizers are on demand there, but conclusions are general and can be extended to optical or microwave frequency ranges as well.

The paper is organized as follows. After briefly mentioning the idea of the elliptical polarization conversion in Sect. 2, we perform the theoretical analysis of the metamaterial polarization converter with the help of the transmission line theory in Sect. 3. The upper limits of the conversion efficiency are derived here. We optimize and numerically characterize few examples of the circular polarizers designs in the transmission and reflection configurations in Sect. 4. Section 9 ends up the paper.

2 Methodology: elliptical polarization

As we mentioned in Introduction, there are two principle strategies to convert a linear polarization into an elliptical one. Assume a wave propagating along the z-axis (Fig. 1) with amplitude $E_0 = 1$ for simplicity. One way is to use a bianisotropic metamaterial with two elliptical eigenpolarizations, which have different absorption or reflection coefficients (elliptical dichroism). An incident linear wave splits into elliptical eigenwaves upon the incidence on a metamaterial slab, and the eigenwave with the higher transmission coefficient will manifest the output polarization. However, such polarization converter provides at the output only a fixed specific elliptical polarization and a part of the wave intensity is lost by default in absorption or poor coupling (reflection).

Another strategy, which is more flexible, is to split the incoming wave into two nonparallel linearly polarized eigenwaves in a birefringent material. Assume the perfect transmission of both polarizations. The waves propagating with different phase velocities in the medium gain relative phase shift $\Delta\phi$. At the output port we sum them up together. In general, an arbitrary angle between linear polarizations along with arbitrary $\Delta\phi$ (except 0 and 180°) results in an elliptical polarization [29]. From the practical point of view, however, the most convenient case is to use two orthogonal linear polarizations E_x and E_y with the phase shift $\Delta\phi = 90°$ (see Fig. 1). Then, being combined at the output, two waves

$$E_x = A_x \cos(\omega t), \quad E_y = A_y \cos(\omega t + \Delta\phi), \tag{1}$$

give an elliptical wave described by the equation

$$\left(\frac{E_x}{A_x}\right)^2 + \left(\frac{E_y}{A_y}\right)^2 = 1. \tag{2}$$

The principle axes of the ellipse in Eq. (2) are along the x- and y-directions.

Introducing angle β between the linear incoming polarization and the x-axis (see Fig. 1) defines waves' amplitudes A_x, A_y and ellipticity k (we assume perfect transmission $|t_x| = |t_y| = 1$ for simplicity):

$$A_x = \cos\beta, \quad A_y = \sin\beta, \quad k = \frac{A_x}{A_y} = \cot\beta. \tag{3}$$

Changing angle β leads to the changes in both amplitudes and ellipticity, but keeps the ellipse orientation. Rotating the polarizer and, therefore, the coordinate system xy connected to it, together with the incoming wave polarization with respect to the fixed coordinate system $x'y'$ on angle α (see Fig. 1) allows for changing the ellipse orientation.

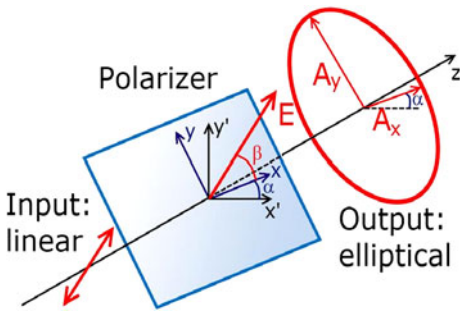

Fig. 1 Operation principle of the polarization converter. An incoming linearly polarized wave is converted into an elliptically polarized. Rotating the linear incoming polarization with respect to polarizer (angle β) we can obtain any polarization from linear to circular. Rotating the device together with the input polarization (angle α) we can change the orientation of the output ellipse

In such a way, we can obtain any elliptical polarization starting from linear ($A_x = 0$ or $A_y = 0$) to circular ($A_x = A_y$) with right or left rotation direction and with any ellipse orientation. We should note that in reality the transmission through a device cannot be 100 % due to imperfections, but in order to cover the whole range of possible polarizations we just need the equality of the x- and y-polarized wave transmissions.

3 Transmission line analysis

The previous section gives the general strategy for obtaining any elliptical polarization out of an incoming linear one. Now, we are looking for the guidelines for the polarizer design. It is desirable for the practical applications (and also fabrication-wise) to have a thin device, so we assume that our polarization converter is a thin layer of a metamaterial with thickness $H \ll \lambda$.

To analyze the electromagnetic (optical) properties of the required metamaterial we employ the transmission-line (TL) approach [30, 31]. In the TL theory an x-polarized plane wave propagating in dielectric with the refractive index n is equivalent to the fundamental mode of a rectangular dielectric waveguide with the perfect electric (x-walls) and perfect magnetic(y-walls) boundaries. The relative (to the free-space impedance $Z_0 = 120\ \pi\ \Omega$) wave impedance $\eta = \sqrt{\mu/\varepsilon}$, where μ and ε are the relative magnetic permeability and electric permittivity of the material. For non-magnetic dielectrics $\mu = 1$, and $\eta = 1/n$. If we consider a plane interface between two non-magnetic dielectrics with refractive indices n_1 and n_2, then the reflection r and transmission t coefficients of the normally incident plane wave are expressed through the wave impedances $\eta_1 = 1/n_1$ and $\eta_2 = 1/n_2$

$$t = \frac{\frac{2}{\eta_1}}{\frac{1}{\eta_1} + \frac{1}{\eta_2}}, \tag{4}$$

$$r = \frac{\frac{1}{\eta_1} - \frac{1}{\eta_2}}{\frac{1}{\eta_1} + \frac{1}{\eta_2}}. \tag{5}$$

If we add a thin (much thinner than the wavelength) layer of a metamaterial with electrical impedance Z_M at the interface between two dielectrics it will act as a shunt (Fig. 2a). The equivalent normalized impedance of the shunt is $\eta_M = (Z_M/Z_0)(a_y/a_x)$ (Fig. 2b), where a_x, a_y are the periods of the unit cell of the metamaterial. The transmission t, reflection r, transmittance T and reflectance R of the wave normally incident from the left side are

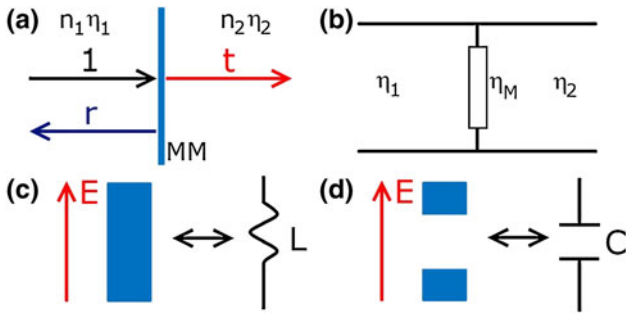

Fig. 2 Reflection and transmission of a plane wave incident on the metamaterial interface between two dielectrics (**a**) is equivalent to reflection and transmission of the wave in the connected transmission lines with different impedances η_1 and η_2 and shunted with a load η_M (**b**). In the lossless metamaterial a metallic wire along the electric field is an analogue of an inductor (**c**), while a dielectric gap between two metal parts is equivalent to a capacitor (**d**)

$$t = \frac{\frac{2}{\eta_1}}{\frac{1}{\eta_1} + \frac{1}{\eta_2} + \frac{1}{\eta_M}}, \tag{6}$$

$$r = \frac{\frac{1}{\eta_1} - \frac{1}{\eta_2} - \frac{1}{\eta_M}}{\frac{1}{\eta_1} + \frac{1}{\eta_2} + \frac{1}{\eta_M}}, \tag{7}$$

$$T = \frac{\eta_1}{\eta_2}|t|^2, \tag{8}$$

$$R = |r|^2. \tag{9}$$

In the extreme case of $\eta_M = \infty$ (no metamaterial layer) expressions reduce to Fresnel's formulas (4) and (5). If $\eta_M = 0$ (short circuit, which is equivalent to a perfectly conducting mirror), we get $t = 0$, $r = -1$.

To design a metamaterial-based circular polarizer we target the equal transmittances/reflectances for x- and y-polarizations and phase difference $\Delta\phi = 90°$. First, we formulate the requirements on the metamaterial impedance η_M accordingly to formulas (6)–(9). Then we analyze transmittance and reflectance (depending on configuration) from the point of view of maximal values which can be obtained by adjusting impedances. Then we guess the geometry to get the designated η_M. The simple rules bridging the transmission line theory and optics are that the inductive impedance requires the employment of a metallic wire along the electric field (Fig. 2c), while the capacitive impedance means a dielectric gap between metallic parts (Fig. 2d). Finally, the fine tuning of the design geometry is done with the help of numerical optimization in CST Microwave Studio [32].

We begin our theoretical analysis assuming that the metamaterial is made of a perforated perfect conductor film that is a fairly good approximation for metals in the microwave and THz range. Thus, the metamaterial impedance is

fully reactive (pure imaginary) $\eta_M = -ix$, where x is an effective reactance. Since we use the optical notation for the time exponential $\exp(-i\omega t)$, positive x means predominantly inductive impedance $\eta_M = -i\omega L$ ($x = \omega L$), while negative $x = -1/(\omega C)$ means predominantly capacitive impedance $\eta_M = i/(\omega C)$. Then the transmission and reflection coefficients (6–9) are

$$t = \frac{\frac{2}{\eta_1}}{\frac{1}{\eta_1}+\frac{1}{\eta_2}+\frac{i}{x}} = \frac{2}{1+\gamma+i\xi}, \tag{10}$$

$$r = \frac{\frac{1}{\eta_1}-\frac{1}{\eta_2}-\frac{i}{x}}{\frac{1}{\eta_1}+\frac{1}{\eta_2}+\frac{i}{x}} = \frac{1-\gamma-i\xi}{1+\gamma+i\xi}, \tag{11}$$

$$T = \frac{\frac{4}{\eta_1\eta_2}}{\left(\frac{1}{\eta_1}+\frac{1}{\eta_2}\right)^2+\frac{1}{x^2}} = \frac{4\gamma}{(1+\gamma)^2+\xi^2}, \tag{12}$$

$$R = \frac{\left(\frac{1}{\eta_1}-\frac{1}{\eta_2}\right)^2+\frac{1}{x^2}}{\left(\frac{1}{\eta_1}+\frac{1}{\eta_2}\right)^2+\frac{1}{x^2}} = \frac{(1-\gamma)^2+\xi^2}{(1+\gamma)^2+\xi^2}. \tag{13}$$

where $\gamma = \eta_1/\eta_2 = n_2/n_1$ and $\xi = \eta_1/x$.

The phases of reflected and transmitted waves are defined through the tangent functions:

$$\tan\phi_t = -\frac{\xi}{1+\gamma}, \tag{14}$$

$$\tan\phi_r = -\frac{2\gamma}{1-\gamma^2-\xi^2}. \tag{15}$$

3.1 Metamaterial layer: transmission configuration

Consider a single metamaterial layer in the transmission configuration [7, 10, 15]. From the requirement of equal transmittance $T_x = T_y$ we find that the reactance for the x- and y-polarizations should be equal in absolute values $|\xi_x| = |\xi_y|$. Among the real solutions $\xi_x = \pm\xi_y$ the "+" solution leads to the same phase advance for both polarization, and, therefore, must be excluded. So, the only suitable solution is $\xi_x = -\xi_y$. That means in the simplest case that the impedance of the metamaterial should be inductive for one polarization and capacitive for another.

Consequently, the transmission phase tangents $\tan\phi_{t,x} = -\tan\phi_{t,y}$. Since the phase difference should be 90°, the product of their tangents is $\tan\phi_{t,x}\tan\phi_{t,y} = -1$. Therefore, $\tan^2\phi_{t,x} = 1$ and

$$\tan\phi_{t,x} = -\frac{\xi_x}{1+\gamma} = \pm 1. \tag{16}$$

Let us, for certainty, select the positive solution for x-polarization then the negative solution will correspond to y-polarization, thus reactances are

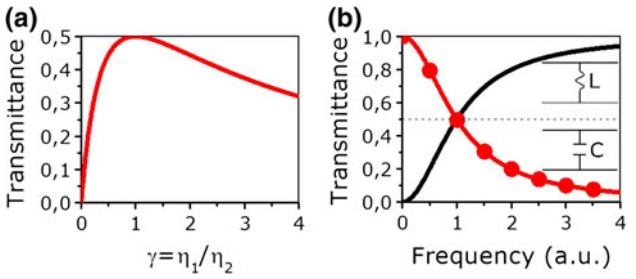

Fig. 3 **a** The dependence of transmittance on $\gamma = \eta_1/\eta_2 = n_2/n_1$ shows that the maximal transmittance $T = 0.5$ is reached when $\gamma = 1$. **b** Positive and negative ξ of a metamaterial is analogous to the high- and low-frequency filters, respectively. Being selected in an appropriate way, they can have equal transmittances and a phase difference 90° at the working frequency

$$\xi_x = -\xi_y = (1+\gamma). \tag{17}$$

The transmittance is

$$T = \frac{2\gamma}{(1+\gamma)^2}, \tag{18}$$

The maximal value of transmittance $T_{max} = 0.5$ can be reached for $\gamma = \eta_1/\eta_2 = 1$ (Fig. 3a) that means the metamaterial is placed between the same surrounding materials. Physically this means either a metallic membrane suspended in air [33] or a metamaterial coated with dielectric with the same refractive index as of the substrate.

A metamaterial satisfying this solution should exhibit inductive properties for x-polarization (metallic wires along the x-axis) and capacitive for y-polarization (dielectric gapes orthogonally to the y-axis). In the transmission line analogy this is a high-frequency filter for the x- and low-frequency filter for the y-polarization (Fig. 3b). In the simplest case, such polarization converter can consist of a set of metallic stripes or wires along the x-axis.

3.2 Metamaterial layer: reflection configuration

Now we consider a single metamaterial layer in the reflection regime [19]. Similar to the transmission case reflectance for both linearly polarized waves should be the same $R_x = R_y$. So, the reactances should be identical in absolute values $|\xi_x| = |\xi_y|$. Analogous to the transmission regime analysis we come to conclusion that $\xi_x = -\xi_y$, and then reactance ξ_x can be extracted from the expression for the reflection phase (15)

$$\tan\phi_{r,x} = -\frac{2\xi_x}{1-\gamma^2-\xi_x^2} = \pm 1, \tag{19}$$

which is a quadratic equation for ξ_x. Selecting the positive sign for the x-polarization in Eq. (19), we obtain

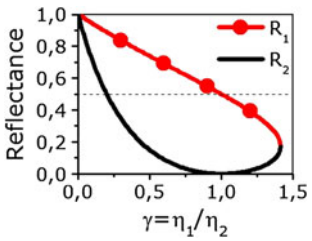

Fig. 4 There are two solutions for $\gamma = \eta_1/\eta_2 = n_2/n_1 < \sqrt{2}$. Both of them have reflectances less than 0.5 for $\gamma > 1$ and can have large reflectance $R \approx 1$ for $\gamma \ll 1$. Physically this means an incidence from the material with a refractive index $n_1 \gg n_2$

$$\xi_x^2 - 2\xi_x - 1 + \gamma^2 = 0. \tag{20}$$

The analysis of this quadratic equation reveals that there are no solutions for $\gamma > \sqrt{2}$, so it is not possible to reach the phase difference 90° between polarizations with any metamaterial. For $\gamma < \sqrt{2}$ the solutions for reactances for both polarizations are

$$\xi_{x,1} = -\xi_{y,1} = 1 + \sqrt{2 - \gamma^2}, \tag{21}$$

$$\xi_{x,2} = -\xi_{y,2} = 1 - \sqrt{2 - \gamma^2}. \tag{22}$$

The corresponding reflectances

$$R_1 = \frac{2 - \gamma + \sqrt{2 - \gamma^2}}{2 + \gamma + \sqrt{2 - \gamma^2}}, \tag{23}$$

$$R_2 = \frac{2 - \gamma - \sqrt{2 - \gamma^2}}{2 + \gamma - \sqrt{2 - \gamma^2}}, \tag{24}$$

are shown in Fig. 4. For both solutions reflectance is less than 0.5 for $1 < \gamma < \sqrt{2}$. For $\gamma = 1$ the first solution (21) coincides with the maximal transmission solution (17). In this case the converter works simultaneously in reflection and transmission regimes, giving 50 % reflectance and 50 % transmittance.

Note, however, that the ratio γ can be less than 1. It can happen if the second dielectric has smaller refractive index than the first one, so the incidence should occur, for example, through a high-dielectric substrate. With such impedances reflectance can be larger than 0.5, and even equal to 1 for $\gamma = 0$. It is, however, not possible to use such high-dielectric substrates due to natural limitations on the material properties and also due to a poor wave in-coupling to a high-dielectric substrate from air. For a practically important case of a silicon substrate in air, $\gamma \approx 0.3$ that corresponds to the reflectance $R_1 \approx 0.84$ and $R_2 \approx 0.36$. So, in contrary to the transmission regime with the maximal polarization conversion up to 50 %, it is possible to achieve larger power conversions in the reflection configuration.

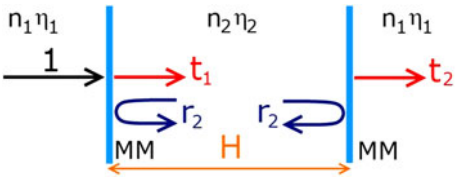

Fig. 5 Two identical metamaterial layers separated with a dielectric form a Fabry–Perot resonator

3.3 Two metamaterial layers: 100 % conversion efficiency in transmission

The theoretical limit for the conversion efficiency for a single layer metamaterial is 50 %. We can, however, expect larger efficiency applying two layers of metamaterial separated with a dielectric spacer [7, 13, 14, 34]. Even very reflective mirrors arranged as a Fabry–Perot resonator can give transmittance close to 1. Let us consider a symmetric configuration shown in Fig. 5, namely, two thin identical metamaterial layers separated with a dielectric n_2 and having a dielectric n_1 from the left and from the right.

The transmission through a Fabry–Perot resonator is [35]

$$t = \frac{t_1 t_2 \exp(i\Phi)}{1 - r_2 \exp(i2\Phi)}, \tag{25}$$

where $\Phi = k_0 n_2 H$, H is the thickness of the dielectric spacer between metamaterial layers, n_2 is its refractive index, k_0 is the free-space wavenumber and the meaning of the reflection and transmission coefficients t_1, r_2, t_2 is clear from Fig. 5.

Through a tedious analysis we found that equal transmittances for the x- and y-polarizations occur for the same condition for the metamaterial impedance $\xi_x = -\xi_y$ as for a single layer.

The tangent of the transmission phase is

$$\tan\phi_t = -\frac{\xi(\gamma - \sin\Phi)}{\gamma - \frac{1}{2}(1 + \gamma^2 - \xi^2)\sin\Phi}. \tag{26}$$

The condition for the 90° phase difference $\tan\phi_x \tan\phi_y = -1$ leads to a quadratic equation for ξ_x. It has two solutions (note that $\xi_{x,1} = -\xi_{y,1}$, $\xi_{x,2} = -\xi_{y,2}$)

$$\xi_{x,1} = 1 - \gamma\cot\Phi + \sqrt{2 + \gamma^2(1 + \cot^2\Phi)} \tag{27}$$

$$\xi_{x,2} = 1 - \gamma\cot\Phi - \sqrt{2 + \gamma^2(1 + \cot^2\Phi)} \tag{28}$$

with the corresponding transmittances

$$T_1 = \frac{1}{2}\frac{1}{(\sqrt{1 + 2w^2} - w)^2}, \tag{29}$$

$$T_2 = \frac{1}{2}\frac{1}{(\sqrt{1 + 2w^2} + w)^2}, \tag{30}$$

where $w = \sin\Phi/\gamma = \frac{\eta_2}{\eta_1}\sin(k_0 n_2 H) = \frac{n_1}{n_2}\sin(k_0 n_2 H)$.

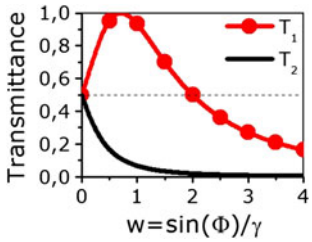

Fig. 6 There are two solutions for the metamaterial reactances. The first solution (27) can give the transmittance up to 100 %, while the transmittance for the second solution (28) cannot exceed 50 %

The transmittance for the second solution (Fig. 6) is always $T_2 < 0.5$. However, choosing the first solution it is possible to achieve the full transmission: $T_1 = 1$ for $w = 1/\sqrt{2}$. That imposes the condition for the spacer thickness H

$$\sin(k_0 n_2 H) = \gamma/\sqrt{2} = \frac{n_2}{n_1\sqrt{2}}. \tag{31}$$

In the case when $n_2/n_1 > \sqrt{2}$, there are no real solutions for Eq. (31), and it is not possible to achieve even theoretically the 100 % transmittance. Such situation can happen if the metamaterials layers are separated with a high refractive index dielectric. Nevertheless, by coating the metal layers with additional dielectric (see, for example the meanderline structure in [7]) it is always possible to reduce the ratio $\gamma = n_2/n_1$ and improve the transmission characteristics.

3.4 Metamaterial layer above ground plane: 100 % conversion efficiency in reflection

Despite a larger conversion efficiency in the reflection configuration comparing to the transmission regime, the reflectance is not 100 % (see Sect. B). Moreover, the incidence from the high-dielectric material side requires preliminary in-coupling to a substrate and therefore some power backscattering. It is, however, possible to overcome these challenges and reach up to 100 % reflectance for the incidence from air using a metal mirror (ground plane) below the metamaterial layer (Fig. 7) [17, 18, 20, 21].

Physically such system is a kind of the Fabry–Perot resonator with a perfect mirror ($r_3 = -1 = \exp(i\pi)$) and a metamaterial mirror (see Fig. 7). The total reflectance from this system is [35]:

$$r = r_1 - \frac{t_1 t_2}{\exp(-i2\Phi) + r_2}, \tag{32}$$

where $\Phi = k_0 n_2 H$ and the meaning of the reflection and transmission coefficients r_1, t_1, r_2, t_2 is clear from Fig. 7.

For the case of the perfect ground plane the reflectance is unitary $R = |r|^2 = 1$ for both polarizations at any frequency. The wave has simply no other options than to be reflected. A tedious analysis of the reflection phase ϕ_r shows that

$$\tan\phi_r = \frac{2(\xi + \gamma\cot\Phi)}{(\xi + \gamma\cot\Phi)^2 - 1}. \tag{33}$$

Requirement $\tan\phi_{r,x}\tan\phi_{r,y} = -1$ ensures the 90° phase difference between polarizations. That leads to a parametric quadratic equation

$$v_x^2 v_y^2 - v_x^2 - v_y^2 + 4v_x v_y + 1 = 0, \tag{34}$$

where $v_x = \xi_x + \gamma\cot\Phi$, $v_y = \xi_y + \gamma\cot\Phi$. This quadratic equation reduces to two independent cases of linear equations

$$(v_x + 1)(v_y - 1) = -2, \tag{35}$$

$$(v_x - 1)(v_y + 1) = -2. \tag{36}$$

So, for each specific v_x there are two solutions that give the required converter functionality

$$v_{y,1} = 1 - \frac{2}{v_x + 1}, \tag{37}$$

$$v_{y,1} = -1 - \frac{2}{v_x - 1}. \tag{38}$$

It means that for any specific thickness H for any given x-polarization reactance ξ_x there exists a real-valued y-polarization reactance ξ_y. Moreover, in contrary to all previous cases (transmission and reflection from a single metamaterial layer or transmission through a double layer), the reactances ξ_x and ξ_y are not obliged to be of different signs. They can be both positive or negative. It is possible to use a fully inductive (or capacitive) metamaterial for both polarizations, for example, a two-dimensional wire grid (or patches).

We note that, in principle, we have four variables that we can change in design: metamaterial impedances ξ_x and ξ_y, dielectric impedances ratio γ and the thickness of the second dielectric H. The simplest tuning can be done by the dielectric thickness H optimization. An important question is whether there can be always found the value of H for any given pair of ξ_x, ξ_y.

For the first (35) and second (36) solutions we have equations for $u = \gamma\cot\Phi$

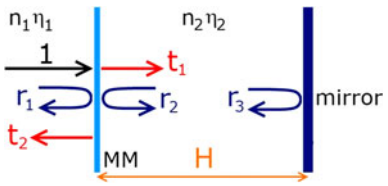

Fig. 7 Metamaterial layer above a ground plane has 100 % reflectance for any metamaterial impedance

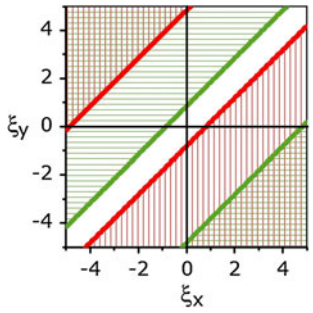

Fig. 8 The graphical representation of the allowed pairs of metamaterial reactances ξ_x, ξ_y that give a solution to the dielectric thickness H. The first and second solution are marked with *vertical red* and *horizontal green lines*, respectively. There exist areas where two, one and no solutions are possible. Solutions can be of the same sign

$$(\xi_x + 1 + u_1)(\xi_y - 1 + u_1) = -2, \tag{39}$$

$$(\xi_x - 1 + u_2)(\xi_y + 1 + u_2) = -2, \tag{40}$$

which have solutions

$$u_1 = \frac{1}{2}[-(\xi_x + \xi_y) \pm \sqrt{(\xi_x - \xi_y + 2)^2 - 8}], \tag{41}$$

$$u_2 = \frac{1}{2}[-(\xi_x + \xi_y) \pm \sqrt{(\xi_y - \xi_x + 2)^2 - 8}], \tag{42}$$

when conditions

$$|\xi_x - \xi_y + 2| \geq 2\sqrt{2}, \tag{43}$$

$$|\xi_y - \xi_x + 2| \geq 2\sqrt{2}, \tag{44}$$

are satisfied. The graphical representation of allowed ξ_x, ξ_y is shown in Fig. 8. There are values of ξ_x, ξ_y corresponding to two or only one solution for $u = \gamma \cot(k_0 n_2 H)$ and therefore for H. There are also ranges, where apparently no solutions exist. This result is expected since for the case of equal impedances $\xi_x = \xi_y$ no phase difference between polarizations can occur upon reflection.

4 Simulation results

In order to test the abovementioned theoretical findings we developed several polarization converters based on the same unit cell geometry, aiming the THz frequency range around 1 THz. The simulations were done in CST Microwave Studio [32]. We applied the periodic (unit cell) boundary conditions in the x- and y-directions, and open space boundary conditions (perfectly matched layers) in the z-direction. We used silver described with the Drude model ($\epsilon_\infty = 5, \omega_p = 1.37 \times 10^{16}$rad/s, $\gamma = 1.6 \times 10^{13}$Hz)) as metal and silica ($n = 1.5$) in most cases as dielectric. Only in the single layer reflection configuration we used silicon ($n = 3.5$).

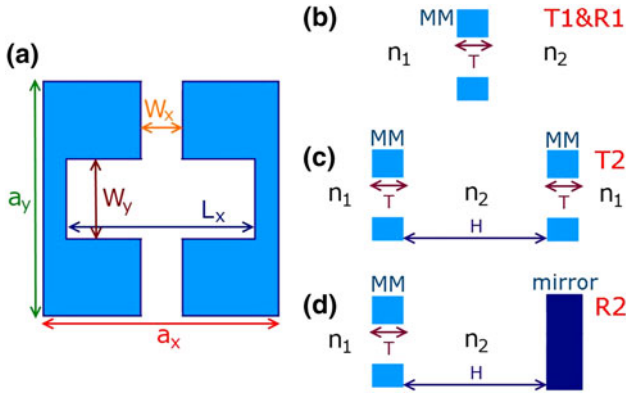

Fig. 9 **a** Metamaterial's unit cell design for polarization converter: view from *top*. *Side view* of the polarizer in the transmission (*T1*) and reflection (*R1*) single layer (**b**), transmission double layers (*T2*) (**c**) and reflection single layer with ground plane (*R2*) (**d**) configurations

Table 1 Design parameters for the polarization converters

Parameter	T1	R1	T2	R2
a_x (μm)	75	60	105	30
a_y (μm)	75	50	65	30
L_x (μm)	72	55	103	18
W_x (μm)	19	10	50	7.5
W_y (μm)	30	17	40	8
T (μm)	1	1	1	1
H (μm)	–	–	30	55

As we mentioned before, the simplest shape for the simultaneously x-polarization capacitive and y-polarization inductive metamaterial is a stripe grid with dielectric gaps in the $x$direction. To obtain more flexibility in the geometrical parameters we modified the stripes to the unit cell shown in Fig. 9. The geometrical sizes of the characteristic features, optimized for the highest possible transmission or reflection in all four regimes are presented in Table 1. We use the following designations: T1—single metamaterial layer polarization converter in transmission; R1—single metamaterial layer polarization converter in reflection; T2—double metamaterial layer polarization converter in transmission and R2—single metamaterial layer polarization converter with a ground plane.

The numerical results for the transmittance/reflectance and phase difference between polarizations for different designs (T1, R1, T2 and R2) are shown in Fig. 10. For all designs we demonstrate the polarization conversion close to the theoretical maximum and the phase difference close to 90°. The double layer structure (T2) has the transmittance (Fig. 10c) almost twice as large as for the single layer (T1) (Fig. 10a). The mirror-based design R2 is, as expected,

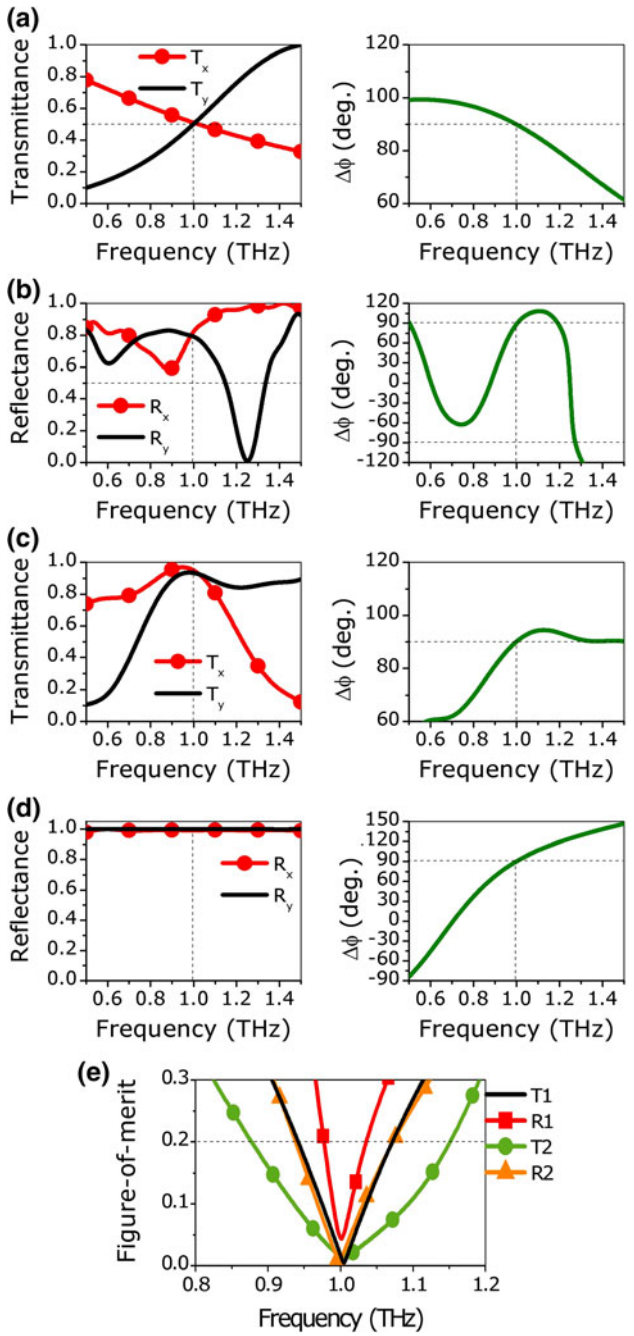

Fig. 10 Transmittance/reflectance and phase difference for designs **a** *T1*, **b** *R1*, **c** *T2*, **d** *R2* are close to the theoretical maxima. **e** Figure of merit FoM < 0.2 shows the converter's bandwidth, which is the largest for the transmission through two metamaterial layers (*T2*) design

Table 2 Parameters of the polarization converters

Design	CE_T (%)	CE_S at 1 THz	$\Delta\nu$ (GHz)	$\Delta\nu_{rel}$
T1	50	50	129	0.129
R1	84	81	57	0.057
T2	100	94	273	0.273
R2	100	99.7	134	0.134

polarization insensitive and achromatic in the whole frequency range (Fig. 10d).

We should mention that both the transmittance/reflectance values and the phase difference influence the conversion efficiency. To account for both influences and to determine the working bandwidth we used the approach established by Rahm et al. [13]. The figure-of-merit (FoM) for the converter, also known as flattening, shows how close the polarization ellipse is to a circle for the input linear polarization incident at 45°. To calculate it one should get a normalized electric field vector at the output $\mathbf{E} = \hat{x}t_x + \hat{y}t_y \exp(i\Delta\phi)$, where $\hat{x}$ and $\hat{y}$ are unit vectors in the corresponding directions. Then, to calculate the angle $\psi = \arg(\mathbf{E}^2)$ and vectors corresponding to ellipse's semi-axis $\mathbf{a_1} = Re(\mathbf{E}\exp(-i\psi/2))$ and $\mathbf{a_2} = Im(\mathbf{E}\exp(-i\psi/2))$. Eventually, FoM $= 1 - (|\mathbf{a_2}|/|\mathbf{a_1}|)^{\pm 1}$. Plus or minus should be chosen depending on whether $\mathbf{a_1}$ or $\mathbf{a_2}$ is the major semi-axis. The figure-of-merit close to 0 shows that the polarizer works well. The working range is defined as the frequency range, where FoM < 0.2 [13]. The steepest phase difference profile is observed for the R1 design, what is reflected in the narrowest bandwidth (Fig. 10e). The broadest FoM is observed with the T2 design due to the flatness of the phase difference spectral profile. The main parameters of the polarizers: theoretical conversion efficiency (CE_{T), conversion efficiency extracted from simulations (CE_{S), bandwidth ($\Delta\nu$) and relative bandwidth ($\Delta\nu_{rel} = \Delta\nu/1\text{THz}$) are presented in Table 2.

5 Discussion and conclusions

We have performed the general analysis of a metamaterial-based polarization converter capable to transform a linearly polarized incident wave into elliptically polarized with any desired ellipticity and ellipse orientation. It is applicable to any thin-film (thickness $\ll$ wavelength) polarization converter with linear eigenpolarizations. We claim that a polarization converter should not necessarily be based on resonant particles (the resonance usually means an increased absorption), i.e. detuned dipoles, resonant apertures, etc., but rather on special relations between impedances for eigenpolarizations. Such impedances can correspond to the resonant or non-resonant metamaterials. The latter case usually provides a broader operation bandwidth. Even though it is not possible to remove completely parasitic capacitance and inductance, so resonances always exist. However, by a proper design we can tune the metamaterial to the frequency far away from an undesirable resonance.

As soon as the clear identification of the impedances and geometrical parameters of elements exist it is not a problem to rescale the metamaterial polarization converter to

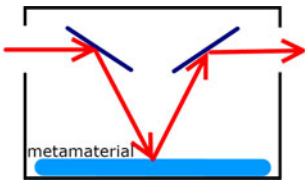

Fig. 11 The reflection polarizer can easily be converted into the transmission polarizer with the help of additional mirrors. For that the metamaterial layer should preserve its functionality for the incidence at small angles

virtually any range of electromagnetic waves. In particular, we have successfully checked the scaling of the T1 design up to the telecom frequencies.

We have also showed numerically that a single type of the metamaterial unit cell can be used for any converter configuration: all four our designs T1, R1, T2, R2 are based on the same type of a unit cell differing only by optimized values of characteristic features. The one-layer transmission configuration T1 has been proved to have theoretical limit of conversion efficiency 50 %. Previously 50 [10], 45 [7] and 44 % [15] were reported. The maximal reflectance approaches 80–90 % for a single metamaterial layer with realistic dielectric properties (silicon substrate), however the steep spectral dependence of the phase shifts reduces the working range of the polarizer. Resonant antennas system was reported to provide 40 % in reflectance [19]. We have demonstrated that a linear-to-circular polarization converter exhibits better performance (with the upper limit 100 % transmittance or reflectance) when two metamaterial layers are involved. The broadest working range 273 GHz is found for the transmission double layer configuration T2. The reported results for the transmittance for such systems (74 [13], 25 [14], 80 [7] and 50 % [34]) can theoretically be improved. The case of the metamaterial above a ground plane can also be classified as double-layer system, since due to the presence of the mirror plate the wave passes twice through the metamaterial layer. Almost 100 % conversion efficiency was reported: 96 [21], $\sim$100 % [20] and [17]. The important advantage of the reflection design with a ground plate is that the requirements for the impedance values are rather softened, which can facilitate greatly the design and fabrication of the structure. Even though the transmission configuration is conventionally preferable for the real life experiments, we should note that the reflection polarizer configuration can be easily converted into transmission one with the help of additional mirrors (Fig. 11).

We believe that our general approach will become a useful tool for the metamaterial-based polarization converters design and development.

Acknowledgments The authors acknowledge P. U. Jepsen and A. Strikwerda for useful discussions. A. A. acknowledges financial support from the Danish Council for Technical and Production Sciences through the GraTer (11-116991) Project.

References

1. P.U. Jepsen, D.G. Cooke, M. Koch, Terahertz spectroscopy and imaging - modern techniques and applications. Laser Photonics Rev. **5**(1), 124–166 (2011)
2. T. Kleine-Ostmann, T. Nagatsuma, A review on terahertz communications research. J. Infrared Millim. Terahertz Waves **32**(2), 143–171 (2011)
3. M. Tonouchi, Cutting-edge terahertz technology. Nat. Photonics **1**(2), 97–105 (2007)
4. D. Molter, G. Torosyan, G. Ballon, L. Drigo, R. Beigang, Step-scan time-domain terahertz magneto-spectroscopy. Opt. Express **20**(6), 26163–26168 (2012)
5. J.B. Masson, G. Gallot, Terahertz achromatic quarter-wave plate. Opt. Lett. **31**(2), 265–267 (2006)
6. T. Arikawa, X. Wang, A.A. Belyanin, J. Kono, Giant tunable faraday effect in a semiconductor magneto-plasma for broadband terahertz polarization optics. Opt. Express **20**(17), 19484 (2012)
7. A.C. Strikwerda, K. Fan, H. Tao, D.V. Pilon, X. Zhang, R.D. Averitt, Comparison of birefringent electric split-ring resonator and meanderline structures as quarter-wave plates at terahertz frequencies. Opt. Express **17**(1), 136–149 (2009)
8. S.C. Saha, Y. Ma, J.P. Grant, A. Khalid, D.R.S. Cumming. Imprinted terahertz artificial dielectric quarter wave plates. Opt. Express **18**(12), 12168–12175 (2010)
9. A. Drezet, C. Genet, T. Ebbesen, Miniature plasmonic wave plates. Phys. Rev. Lett. **101**(4), 1–4 (2008)
10. J.Y. Chin, M. Lu, T.J. Cui, Metamaterial polarizers by electric-field-coupled resonators. Appl. Phys. Lett. **93**(25), 251903 (2008)
11. J.Y. Chin, J.N. Gollub, J.J. Mock, R. Liu, C. Harrison, D.R. Smith, T.J. Cui, An efficient broadband metamaterial wave retarder. Opt. Express **17**(9), 7640–7647 (2009)
12. X.G. Peralta, E.I. Smirnova, A.K. Azad, H.-T. Chen, A.J. Taylor, I. Brener, J.F. O'Hara, Metamaterials for thz polarimetric devices. Opt. Express **17**(2), 773–783 (2009)
13. P. Weis, O. Paul, C. Imhof, R. Beigang, M. Rahm, Strongly birefringent metamaterials as negative index terahertz wave plates. Appl. Phys. Lett. **95**(17), 171104 (2009)
14. T. Li, S.M. Wang, J.X. Cao, H. Liu, S.N. Zhu, Cavity-involved plasmonic metamaterial for optical polarization conversion. Appl. Phys. Lett. **97**(26), 261113 (2010)
15. A. Roberts, L. Lin, Plasmonic quarter-wave plate. Opt. Lett. **37**(11), 1820–1822 (2012)
16. W. Sun, Q. He, J. Hao, L. Zhou, A transparent metamaterial to manipulate electromagnetic wave polarizations. Opt. Lett. **36**(6), 927–929 (2011)
17. J. Hao, Y. Yuan, L. Ran, T. Jiang, J. Kong, C. Chan, L. Zhou, Manipulating electromagnetic wave polarizations by anisotropic metamaterials. Phys. Rev. Lett. **99**(6), 1–4 (2007)
18. J. Hao, Q. Ren, Z. An, X. Huang, Z. Chen, M. Qiu, L. Zhou, Optical metamaterial for polarization control. Phys. Rev. A **80**(2), 1–5 (2009)
19. A. Pors, M.G. Nielsen, G.D. Valle, M. Willatzen, O. Albrektsen, S.I. Bozhevolnyi, Plasmonic metamaterial wave retarders in reflection by orthogonally oriented detuned electrical dipoles. Opt. Lett. **36**(9), 1626–1628 (2011)
20. A.C. Strikwerda, R.D. Averitt, K. Fan, X. Zhang, G.D. Metcalfe, M. Wraback, Electromagnetic composite-based reflecting terahertz waveplates. Int. J. High Speed Electr. Syst. (IJHSES) **20**(3), 583–588 (2011)

21. F. Wang, A. Chakrabarty, F. Minkowski, K. Sun, Q.-H. Wei, Polarization conversion with elliptical patch nanoantennas. Appl. Phys. Lett. **101**(2), 023101 (2012)
22. R. Singh, E. Plum, W. Zhang, N.I. Zheludev, Highly tunable optical activity in planar achiral terahertz metamaterials. Opt. Express **18**(13), 13425–13430 (2010)
23. S.X. Li, Z.Y. Yang, J. Wang, M. Zhao, Broadband terahertz circular polarizers with single-and double-helical array metamaterials. J. Opt. Soc. Am. A **28**(1), 19–23 (2011)
24. M. Mutlu, A.E. Akosman, A.E. Serebryannikov, E. Ozbay, Asymmetric chiral metamaterial circular polarizer based on four u-shaped split ring resonators. Opt. Lett. **36**(9), 1653–1655 (2011)
25. Y. Zhao, M.A. Belkin, A. Alù, Twisted optical metamaterials for planarized ultrathin broadband circular polarizers. Nat. Commun. **3**, 870 (2012)
26. C. Sabah, H.G. Roskos, Design of a terahertz polarization rotator based on a periodic sequence of chiral-metamaterial and dielectric slabs. Prog. Electromagn. Res. **124**, 301–314 (2012)
27. J.K. Gansel, M. Latzel, A. Frolich, J. Kaschke, M. Thiel, M. Wegener, Tapered gold-helix metamaterials as improved circular polarizers. Appl. Phys. Lett. **100**(10), 101109 (2012)
28. C. Caloz, T. Itoh, *Electromagnetic metamaterials: transmission line theory and microwave applications: the engineering approach*. (Wiley-IEEE Press, New York, 2006)
29. J.D. Jackson, *Classical electrodynamics*, vol. 67, (Wiley, New York, 1999)
30. N.J. Cronin, *Microwave and optical waveguides*. (Taylor & Francis, 1995)
31. S. Tretyakov, *Analytical modeling in applied electromagnetics*. (Artech House Publishers, Boston, 2003)
32. CST. Computer simulation technology. http://www.cst.com/
33. R. Malureanu, P.U. Jepsen, S. Xiao, L. Zhou, D.G. Cooke, A. Andryieuski, A.V. Lavrinenko, Fractal Thz metamaterials: design, fabrication and characterisation. Proc. SPIE **7711**, 77110M (2010)
34. D.-H. Kwon, P.L. Werner, D.H. Werner, Optical planar chiral metamaterial designs for strong circular dichroism and polarization rotation. Opt. Express **16**(16), 11802–11807 (2008)
35. P. Yeh, *Optical waves in layered media*, vol 95. (Wiley, New York, 1988)